43rd IEEE Conference on Decision and Control
December 14-17, 2004
Atlantis, Paradise Island, Bahamas

Nonlinear steering oscillations of motorcycles

Arash Shaeri, David J. N. Limebeer and Robin S. Sharp

Abstract— **Extensive prior modelling of the three dimensional motions of motorcycles, which has depended heavily on linearization for small perturbations from equilibrium "trim" states, is extended to cover large amplitude, nonlinear operating regimes. For a cornering machine, road undulation displacement forcing is shown to be capable of exciting subharmonic and superharmonic responses. A procedure for identifying particular operating conditions that may be expected to yield internal or combination resonances for a baseline modern machine/rider combination is devised. Interesting cases are examined by simulation and the results analysed using short time Fourier transform processing of the output signals. Internal and combination resonances are shown to occur under specially chosen circumstances. A procedure for choosing these special circumstances is described. Some practical implications are also considered.**

I. Introduction

Motorcycles are known to be oscillatory [1]. In straight running, the lateral oscillations, weave and wobble, are the main modes. Typically, the weave mode is well damped at moderate speeds but becomes less so as the speed increases. The natural frequency rises from zero at very low speed to somewhere in the range 2 - 4Hz, depending on the mass and size of the machine, the lowest frequencies corresponding to the heaviest motorcycles. The only properly documented wobble oscillations involve moderate speeds, although there are many anecdotal accounts of wobble at high speeds [2]. Theoretical results indicate that the torsional stiffness of the motorcycle frame at the steering head determines whether a machine will be prone to wobbling at medium speeds (compliant frame), or at high speeds (stiff frame) [3, 4]. The frequency of the mode does not vary much with speed, being governed primarily by the mechanical trail, the front tyre cornering stiffness and the front frame steer inertia [5]. It is normally in the range 6 - 9Hz. The stiff framed machines, being prone to wobbling at high speed, often depend on a steering damper for satisfactory wobble stability, but a steering damper will normally destabilise the high speed weave.

In cornering, the above lateral modes and the in-plane modes associated with tyre deflections and suspension motions become coupled, as first shown in any detail by Koenen [6]. Linearisation for small perturbations from "trim" states allows modes to be calculated, but the mode shapes become complex. Weave couples strongly with bounce and pitch, since their frequencies are similar when they are decoupled and similarly, wobble joins with front suspension action, under cornering. The motorcycle becomes prone to resonate in response to regular road undulation forcing with wavelength and speed matched to the natural vibration frequencies, with moderate lean angles likely to represent worst case conditions [7].

These behavioural properties are known in detail from theoretical work, but there is a broad measure of agreement between theory and practice that allows predictions to be made with confidence.

Since the full motorcycle/rider equations of motion are very complex (too much so to display) and they contain general nonlinear (quadratic, cubic, quartic etc.) terms, the virtual machine and, by implication, real machines, can be expected to demonstrate the behavioural properties of general nonlinear dynamical systems [8]. Such behaviour will naturally be associated with larger amplitudes of vibration, where the nonlinear terms increase in relative importance. It is also implied that they will be associated with unusual operating circumstances.

The experience of the rider will derive mostly from operation near to "trim" states and, insofar as this experience does not encompass nonlinear phenomena, suddenly encountering unlearned situations of changed character is a hazardous possibility. Thus, understanding the nonlinear behaviour of motorcycles is not without implications for motorcycle design, rider training, road maintenance and accident investigation.

In section II, the particular background to the motorcycle model used and the properties of the basic motorcycle/rider system are described. In section III, the spring pendulum is analysed as an example of a nonlinear dynamical system. In section IV, some relevant nonlinear system behaviour is reviewed. In section V, short time Fourier Transform (STFT) processing is discussed. With all the background material then assembled, simulation results showing secondary resonances of the motorcycle/rider system are shown and processed in section VI. In section VII, a procedure for using linear theory to identify especially interesting operating conditions, from a nonlinear dynamics standpoint, is explained. Then in section VIII, simulation results demonstrating internal resonance are shown and processed by STFT techniques, with interpretations. Conclusions are drawn in section IX.

II. Motorcycle model

General motions of motorcycles involve three translations and three rotations of the main frame, steering of the front frame relative to the main one, front and rear suspension freedoms, frame twisting, relative rider upper body motions

This work is supported by the EPSRC.

A. Shaeri, D.J.N. Limebeer and R.S. Sharp are with the Department of Electrical and Electronic Engineering, Imperial College London, London SW7 2AZ, U.K. a.shaeri@imperial.ac.uk, d.limebeer@imperial.ac.uk, robin.sharp@imperial.ac.uk

and wheel spinning. A speed controller may be incorporated and a feedback controller for steer torque is advantageous for stabilising the man/machine system at a desired lean angle, for example, so that steady-state equilibrium conditions can be determined. A model incorporating those main features has been described [7, 9, 10]. It is shown diagrammatically in Fig. 1, in which the masses are represented by circles, each of diameter proportional to the mass involved. Its parameter values are those of a modern sports machine. From the description given before, some parameters have been updated, as shown in the appendix to the paper. Parameter revisions derive from further measurements in the laboratory on the properties of components and further processing of those measurements.

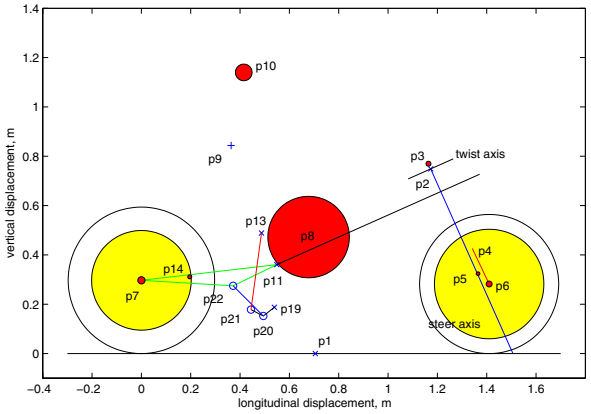


Fig. 1. Diagrammatic motorcycle and rider with masses depicted by circles each with diameter proportional to mass.

The model is written in the symbolic multibody software system AUTOSIM^{TM} [11]. The AUTOSIM model file can be loaded in either of two ways, linear or nonlinear. In the latter case, a simulation program results. Steering torque feedback control can be included or omitted by setting the controller gains appropriately. Among other things, the simulation program, with steering control, can be run to find equilibrium cornering states, typically involving a fixed target lean angle and a slowly ramping target speed. In linear form, the system is symbolically linearised, for small perturbations about a general "trim" condition, and a MATLAB "M" file is written, to set up the linear model, with no steering feedback control, in state space form. The symbolic MATLAB file can be used to generate root-locus plots corresponding to various trim conditions [1]. The "M" file can also be used to find frequency responses to road undulation forcing, as described in [7].

Root-loci for the standard motorcycle and rider are shown in Fig. 2, for straight running and for sustained lean angles of 15 and 30 degrees. The wobble and weave modes are clearly visible in the ranges 40-55 rad/s and 0-26 rad/s respectively.

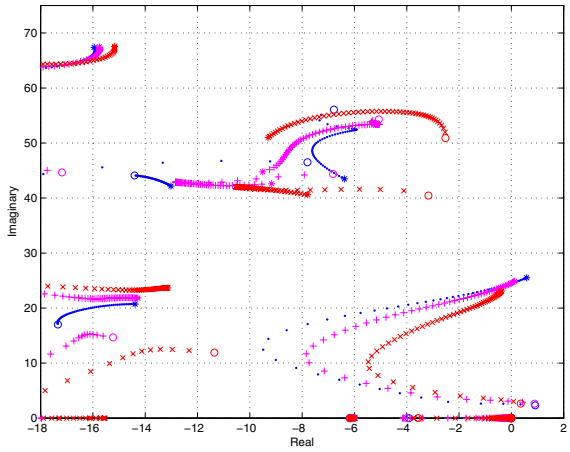


Fig. 2. Root-loci for standard system in straight running (.) and at 15 (+) and 30 ($\times$) degrees lean angle over the speed range 5 ($\circ$) to 75 ($\star$) m/s.

III. Spring Pendulum

Even very simple nonlinear mechanical systems can exhibit rich dynamic behaviour. A standard example of this is the elastic, or spring pendulum [8]. As shown in Figure 3, this system may also be subject to vertical displacement forcing. Standard processes associated with Lagrange mechanics establish that the equations of motion of this system are:

$$(l+r)\ddot{\theta} + 2\dot{r}\dot{\theta} - \ddot{y}_s sin\theta = -gsin\theta - \frac{d_\theta}{m}\dot{\theta} \qquad (1)$$

and

$$\ddot{r} = -\frac{k}{m}r - \frac{d_r}{m}\dot{r} + (g - \ddot{y}_s)cos\theta + (l+r)\dot{\theta}^2 \qquad (2)$$

where d_r and d_θ are damping factors. These equations can be linearsied around the vertical rest position to yield:

$$\delta\ddot{\theta} = -\frac{g}{l+r_0}\delta\theta \qquad (3)$$

and

$$\delta\ddot{r} = -\frac{k}{m}\delta r \qquad (4)$$

from which one concludes that the linearised system has two uncoupled mode of motion with resonant frequencies $\omega_\theta = \sqrt{\frac{g}{l+r_0}}$ and $\omega_r = \sqrt{\frac{k}{m}}$ for the swing and heave modes respectively.

Referring back to equations (1) and (2), one sees that the swing and the heave modes are linked by the quadratic coupling terms $2\dot{r}\dot{\theta}$ in the case of (1) and $l\dot{\theta}^2$ in the case of (2). The impact of these terms can be established using the Lindstedt-Poincaré method [8]. In this method, we suppose that the solutions of equations (1) and (2) can be expanded as:

$$r(t;\epsilon) = \epsilon r_1(t) + \epsilon^2 r_2(t) + \epsilon^3 r_3(t) + \dots$$
$$\theta(t;\epsilon) = \epsilon\theta_1(t) + \epsilon^2\theta_2(t) + \epsilon^3\theta_3(t) + \dots$$

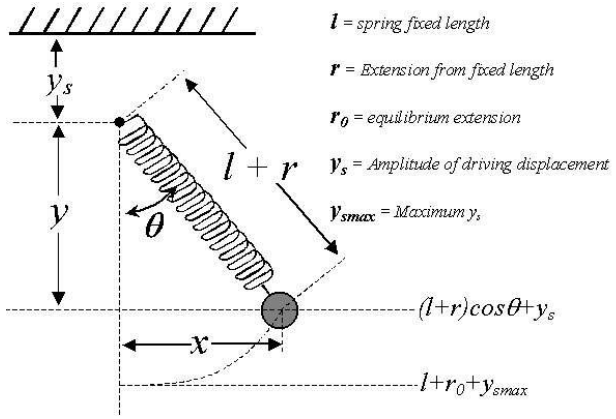


Fig. 3. The spring pendulum.

where ϵ is a small dimensionless parameter and is the order of the amplitude of the motion. We must also introduce a change of variable $\tau = \omega t$ where ω is expanded as:

$$\omega(\epsilon) = \omega_0 + \epsilon\omega_1 + \epsilon^2\omega_2 + \dots$$

After carrying out detailed algebraic manipulations, it can be established that r_1 and θ_1 are the solutions to the linearised equations of motion. More precisely,

$$r_1(\tau) = A_r sin(\omega_r\tau + \phi_r) + r_0$$
$$\theta_1(\tau) = A_\theta sin(\omega_\theta\tau + \phi_\theta)$$

where A_r, A_θ, ϕ_r and ϕ_θ are constants of integration. Further analysis leads to:

$$r_2(\tau) = \frac{gA_\theta^2}{\omega_r^2}\left(1 - \frac{3}{1-4\left(\frac{\omega_\theta}{\omega_r}\right)^2}cos(2\omega_\theta\tau + 2\phi_\theta)\right) + r_0$$

and

$$\theta_2(\tau) = -\frac{\omega_\theta(\omega_\theta + 2\omega_r)}{(l+r_0)\omega_r(\omega_r + 2\omega_\theta)}A_rA_\theta cos((\omega_r+\omega_\theta)\tau + \phi_1)$$
$$-\frac{\omega_\theta(\omega_\theta - 2\omega_r)}{(l+r_0)\omega_r(\omega_r - 2\omega_\theta)}A_rA_\theta cos((\omega_r-\omega_\theta)\tau + \phi_2)$$

The above equations show that when the condition $\omega_r = 2\omega_\theta$ is satisfied, the expansion breaks down indicating an internal resonance condition that will be explained in the next section.

IV. Nonlinear systems behaviour

It is well known that a nonlinear system will display (primary) resonance behaviours when it is externally forced at a frequency that corresponds to the natural frequency of a lightly damped mode of its linearisation. In the case of a system with quadratic nonlinearity, such as the spring pendulum, it is also possible to have subharmonic resonances at $\Omega \approx 2\omega_o$ in which Ω is the external forcing frequency and ω_o is one of its natural frequencies. In such a case, ω_0 is the subharmonic response frequency [8]. In the case of cubic nonlinearities this condition, if it exists, will be governed by $\Omega \approx 3\omega_o$. Superharmonic resonances are also possible, but in this case the conditions will be $\Omega \approx \frac{1}{3}\omega_o$ and $\Omega \approx \frac{1}{2}\omega_o$ for cubic and quadratic nonlinearities respectively. It is shown in [8] that for single degree of freedom systems with quadratic and/or cubic nonlinearities, superharmonic resonance is guaranteed, while subharmonic resonance is only possible when certain system parametric conditions are satisfied. In the case of systems with many degrees of freedom, as is the case with the motorcycle, internal and combination resonances are also possible. In the case of the spring pendulum, internal resonance will be supported by the quadratic coupling terms $2\dot{r}\dot{\theta}$ and $l\dot{\theta}^2$ in the case that $\omega_r = 2\omega_\theta$. In general, these energy exchanges occur by virtue of the existence of special relationships between the modal frequencies and the presence of nonlinear coupling terms, which can be of different orders.

A general nonlinear n-degree-of-freedom system, when linearised, will have n natural frequencies, ω_1, ω_2, ω_3,..., ω_n. Internal resonances can occur if two or more of these frequencies are commensurable, or nearly commensurable [8]. Examples follow: $\omega_2 = 2\omega_1$ for a system with quadratic nonlinearities, $\omega_2 = 3\omega_1$ and $\omega_3 = \omega_1 \pm \omega_2$ for a system with cubic nonlinearities. The strength of the inter-modal coupling depends on the degree to which these commensurability relationships are satisfied and the nature of the nonlinear terms in the governing equations.

With sinusoidal external forcing of frequency Ω, combination resonances can also occur, for example, if $\Omega = \omega_1 \pm \omega_2$ when quadratic nonlinear terms are present. Corresponding conditions apply for systems with higher orders of nonlinearity. See [8] for a detailed analysis and many examples.

V. Short Time Fourier Transform processing

The Fourier Transform is used to analyse the spectral content of a signal. The spectrum of the signal will display the amplitudes of the different frequency components in the signal, but no temporal information about these components can be deduced. In many cases, the spectrum is all that is required, however in the case of signals with time-varying spectral properties, it is also advantageous to have information about the temporal disposition of the various spectral components. In these cases joint time-frequency representations are used to combine temporal and spectral properties of the signal and display them over a time-frequency plane. There are many different time-frequency representations and each has its own charcteristics. Time-frequency representations may be linear or nonlinear. Due to their nature, nonlinear representations suffer from misleading cross-terms which can make the analysis of multi-component signals difficult. In contrast, linear time-frequency representations do not contain cross-terms, but they generally have lower time-frequency resolution. In this paper we will make use of the short time Fourier transform (STFT), which is a simple linear representation.

In mathematical terms, the STFT is defined by

$$S_x(t,\omega) = \int_{-\infty}^{\infty} x(\tau)h(\tau - t)e^{-j\omega\tau}d\tau \qquad (5)$$

in which $x(t)$ is a signal and $h(t)$ is a finite-support window function. The properties of the window function $h(t)$ have a significant effect on the STFT display and has to be selected carefully.

It is not possible to measure a signal's temporal and spectral content simultaneously without some loss of resolution. This is true of all time-frequency methods and is known as the Heisenberg uncertainty principle [12]. In the case of the STFT, the temporal width of the analysis window determines the resolution of the T-F display. A narrow window gives high temporal resolution at the expense of frequency resolution and vice versa (this arises from the fact that $h(t)$ and its Fourier Transform $H(\omega)$ cannot be made arbitrarily narrow simultaneously). The linearity and inherent simplicity of the STFT makes it an attractive option.

When appropriately sampled in both time and frequency, short term spectra may be found via a discrete Fourier transform (DFT) of a sequence $x[k]$. There is no significant information loss if $S_x(t,\omega)$ is replaced with its sampled version $S_x[n,m]$. The usual conditions associated with the Nyquist sampling theorem have to be observed. If $\frac{1}{T}$ and $\frac{1}{F}$ are the time and frequency sampling rates, one obtains $S_x[\frac{n}{T}, \frac{m}{F}]$ in which n and m are time and frequency indexes. More particularly

$$S_x[n,m] = \sum_{k=0}^{T-1} h(nD - k)x(k)e^{-j2\pi k\frac{m}{T}}, \qquad (6)$$

which is a sampled version of equation (5). It is important to note that three different sampling periods have been defined: T_s, the sampling period associated with the input sequence $x[k]$; $\frac{1}{F}$ the frame period for the bandlimited signals at each frequency ω; and $\frac{1}{T}$, the frequency sampling period. The processes behind the proper selection of T_s, F, T and the window function are standard [13].

VI. Secondary Resonance Results

Primary resonance responses can be predicted using linearised models. The study described in [7] is directed to the primary forcing of the wobble and weave modes.

To examine secondary resonances, the nonlinear simulation model has to be employed. The steer angle responses to sinusoidal road displacement forcing at one third of the wobble frequency from the model, for a motorcycle speed of 23m/s and a mean roll angle of 15°, are shown in spectral form in Figure 4. When very low amplitude forcing is used (2.0μm peak-to-peak) the only response is at the forcing frequency. This is the expected linear behaviour. However, when the road forcing amplitude is increased to 0.5cm peak-to-peak, the response spectrum contains a strong component at three times the forcing frequency, constituting a superharmonic resonance. The same steer angle response signal is analysed by the STFT with results shown in Figure 5. It is clear from the time history that the response remains quite small for about 20s and then builds up. In the T-F spectrum, the forcing frequency component is present all the time and a small initial wobble transient can be seen. From approximately 10s, superharmonic response at the wobble frequency can be observed and response components in the second, fourth and fifth harmonics of the forcing frequency can be detected. The steer angle amplitude reaches 6^o peak-to-peak.

Figure 6 shows the yaw-rate response of the machine under cornering with a roll angle of 15^o. The forward speed is 60m/s and the road displacement forcing amplitude 0.5cm peak-to-peak with a frequency of 49.3 rad/s. It is clear that a primary resonance is present immediately as is a subharmonic resonance at 24.7 rad/s. The subharmonic response reaches a higher amplitude than the primary response. From the time response one sees a peak-to-peak yaw-rate that reaches a value of almost 3rad/s. On decreasing the frequency of the road excitation by 10% to 44.4 rad/s, the subharmonic response previously present disappears, Figure 7. Only a weave transient, the primary response and a second harmonic can be observed. The peak-to-peak amplitude of the yaw rate response drops down to 0.3 rad/s, a factor of 10 lower than in the previous case.

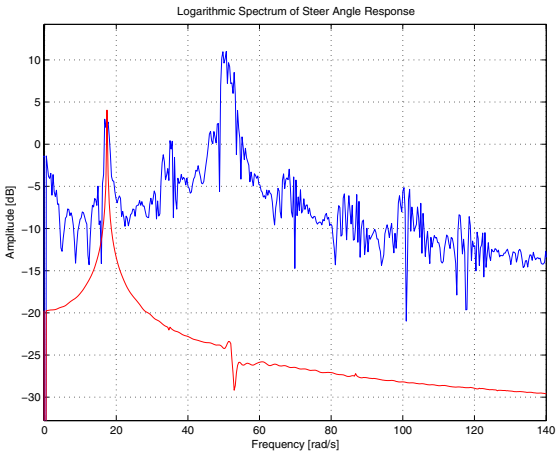


Fig. 4. Logarithmic spectrum of the steer angle response when: speed = 23m/s, roll angle = 15° and $\Omega = \frac{1}{3}\omega_{wo}$.

VII. Operating Conditions for Internal Resonance

As stated in section IV, internal and combination resonances are possible when commensurate relationships exist between natural frequencies of the linearised system. The motorcycle offers many possibilities for such relationships as it varies over a wide range of speed and lean angles. A number of operating conditions exhibiting commensurability were found as follows: the simulation model with stabilising steering torque feedback control was used to find the full range of "trim" states over the speed range

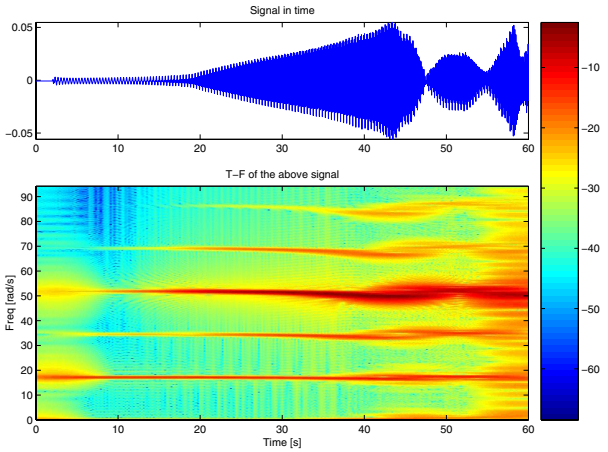


Fig. 5. Logarithmic STFT of steer angle response when: speed = 23m/s, roll angle = 15° and $\Omega = \frac{1}{3}\omega_{wo}$.

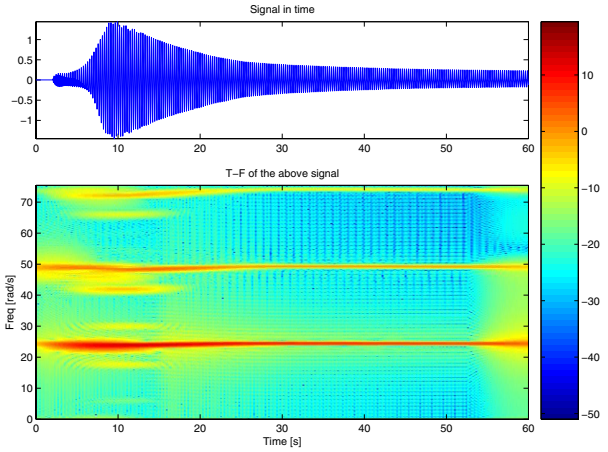


Fig. 6. Logarithmic STFT of yaw rate response when: speed = 60 m/s, roll angle = 15° and $\Omega = 2\omega_{we}$.

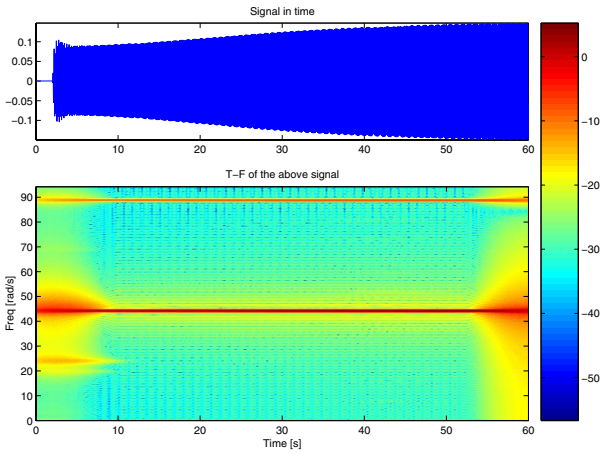


Fig. 7. Logarithmic STFT of yaw rate response when: speed = 60 m/s, roll angle = 15° and $\Omega = 1.8\omega_{we}$ (10% detuning).

for lean angles of 0 (straight running), 15 and 30 degrees. The machine was very slowly accelerated from low to high speed, at a rate too small to significantly influence the equilibrium states. Root-loci, through speed, for each of the 3 lean angles, were then generated and an automated search among the natural frequency results was conducted to detect commensurability, together with low damping factors of the relevant modes.

One case of commensurability between wobble and weave highlighted by the search is shown in Table I. This table corresponds to an operating condition with a forward speed of 54m/s and a roll angle of 15^o. In this case the weave mode frequency is one half of the wobble mode frequency. The steer damping was reduced from its nominal value to make the wobble mode damping factor small and encourage intermodal energy transfer.

TABLE I

OPERATING CONDITIONS SHOWING COMMENSURABILITY

Speed (m/s)	$\frac{\omega_{wo}}{\omega_{we}}$	ω_{wo} **(rad/s)**	ω_{we} **(rad/s)**	ζ_{wo}	ζ_{we}
54	1.9919	47.9480	24.0715	0.0465	0.0465

VIII. INTERNAL AND COMBINATION RESONANCE RESULTS

Figure 8 shows the steer angle response of the cornering motorcycle to road forcing that is tuned into the wobble mode. Due to commensurability, as shown in Table I, the condition $\frac{1}{2}\Omega = \omega_{wo} - \omega_{we}$ is satisfied and so combination resonance is possible.

It is clear that the weave mode is excited, although the primary response comes from the wobble mode at 47.9rad/s. This diagram also shows that the peak-to-peak amplitude of the steer angle is approximately 10^o. The road forcing amplitude is 0.5cm peak-to-peak as in previous cases. Note the strong presence of the second harmonic of the forcing frequency due to the satisfaction of the internal resonance condition outlined in Table I.

In Figure 9, we break the combination resonance condition by changing the forcing frequency to 43.2rad/s, a reduction of 10%. In this case one sees the primary response and a small second harmonic response. The persistent weave mode response has disappeared and there is only an initial transient visible at this frequency. The peak-to-peak amplitude of the steer angle response has dropped to 1.4^o, which is a reduction by a factor of approximately 7.

IX. CONCLUSIONS

Using an advanced motorcycle/rider simulation model, complete with a parametric description of a modern sports motorcycle, the possible occurrence of nonlinear oscillations under road profile forcing of modest amplitude has been demonstrated. The motions have a different character from those previously reported, based on linear analysis.

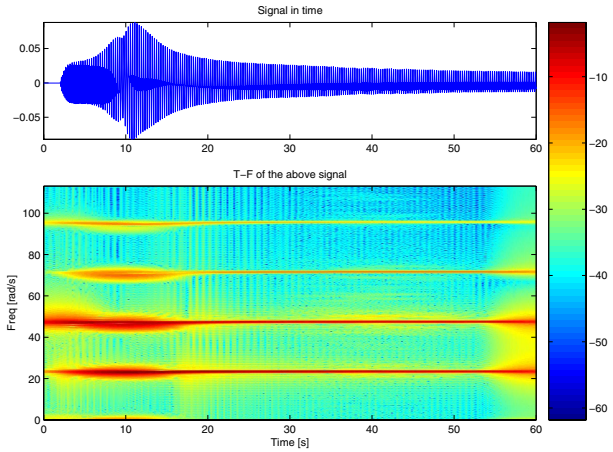


Fig. 8. Logarithmic STFT of steer angle response when: speed = 54 m/s, roll angle = 15°, $\omega_{wo} \approx 2\omega_{we}$ and $\Omega = \omega_{wo}$.

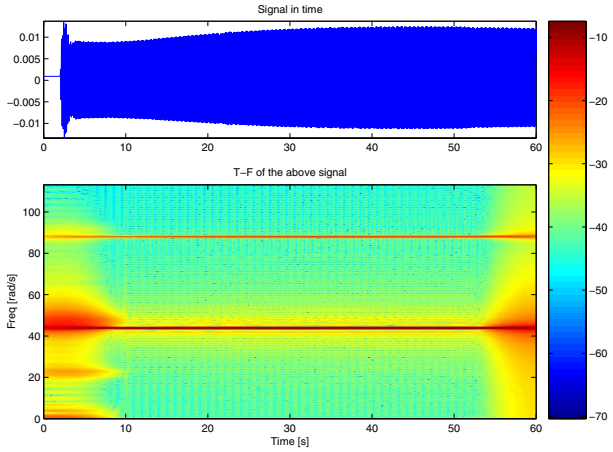


Fig. 9. Logarithmic STFT of steer angle response when: speed = 54 m/s, roll angle = 15°, $\omega_{wo} \approx 2\omega_{we}$ and $\Omega = 0.9\omega_{wo}$ (10% detuning).

The oscillations have been shown to take several forms, including sub-harmonic and super-harmonic vibrations, internal resonance and combination resonance. When these oscillations occur, they can be expected to pose particular problems for riders. Short period Fourier Transform processing has enabled the course of the oscillations to be tracked in terms of time and frequency. Some experience has been gained in relation to choosing the various parameters and window functions in the STFT. In essence, one has to find the best compromise between time and frequency resolution (the uncertainty principle) and this can be achieved via the selection of an appropriate window and window width [13].

Specifically, it has been observed that with adjustments to the steer damping of the machine as described:

1) a superharmonic resonance in wobble could be excited via road displacement forcing at one third of the wobble mode frequency.
2) a subharmonic resonance in weave could be excited via road displacement forcing at twice the weave mode frequency.
3) a combination resonance response could be excited in wobble and weave when the condition $\frac{1}{2}\Omega = (\omega_{wo} - \omega_{we})$ is satisfied in which Ω is the road forcing frequency. This response is supported by the internal resonance condition $\omega_{wo} \approx 2\omega_{we}$.

APPENDIX

Parameter updates with reference to [9], (SI units): Mmain 165.13, Mubr 33.68, Mswg_arm 8, Imnx 11.0854, Imny 22.013, Imnz 14.982, Imnxz -3.691, Iubrx 1.428, Iubry 1.347, Iubrz 0.916, Iubrxz 0.4433, Is_ax 0.02, Is_ay 0.259, Is_az 0.259, z2 -0.7488, x3 1.164, z3 -0.7698, x8 0.6779, z8 -0.4724, z9 -0.8438, x10 0.415, z10 -1.14, z11 -0.3608, z13 -0.4888, z14 -0.3113, z19 -0.1878, x20 0.4946, z20 -0.1522, x21 0.4443, z21 -0.1782, x22 0.3722, z22 -0.2748, f_k 25000, f_c 2134, free_len 0.3435, r_krbd 1e15, f_krbd 1e15.

REFERENCES

[1] R. S. Sharp, "Stability, control and steering responses of motorcycles," *Vehicle System Dynamics*, vol. 35, no. 4–5, pp. 291–318, 2001.

[2] T. Foale. (2002) Motorcycle handling and chassis design – the art and science. [Online]. Available: http://www.tonyfoale.com

[3] R. S. Sharp and C. J. Alstead, "The influence of structural flexibilities on the straight running stability of motorcycles," *Vehicle System Dynamics*, vol. 9, no. 6, pp. 327–357, 1980.

[4] P. T. J. Spierings, "The effects of lateral front fork flexibility on the vibrational modes of straight-running single-track vehicles," *Vehicle System Dynamics*, vol. 10, no. 1, pp. 21–35, 1981.

[5] S. Evangelou and D. Limebeer, "Lisp programming of the "sharp 1971" motorcycle model," 2000, http://www.ee.ic.ac.uk/control/motorcycles.

[6] C. Koenen, "The dynamic behaviour of motorcycles when running straight ahead and when cornering," Ph.D. dissertation, Delft University of Technology, 1983.

[7] D. J. N. Limebeer, R. S. Sharp, and S. Evangelou, "Motorcycle steering oscillations due to road profiling," *Transactions of the ASME, Journal of Applied Mechanics*, vol. 69, no. 6, pp. 724–739, 2002.

[8] A. H. Nayfeh and D. T. Mook, *Nonlinear Oscillations*. NY: Wiley-Interscience, Jan 1979.

[9] R. S. Sharp, S. Evangelou, and D. J. N. Limebeer, "Improved modelling of motorcycle dynamics," in *ECCOMAS Thematic Conference on Advances in Computational Multibody Dynamics*, J. Ambrósio, Ed., Lisbon, July 1–4 2003, MB2003-029 (CD-ROM).

[10] R. Sharp and D. Limebeer, "A motorcycle model for stability and control analysis," *Multibody System Dynamics*, vol. 6, no. 2, pp. 123–142, 2001.

[11] Anon., *Autosim 2.5+ Reference Manual*, Mechanical Simulation Corporation, 709 West Huron, Ann Arbor MI, 1998, http://www.carsim.com.

[12] L. Cohen, "Time-frequency distributions - a review," *Proceedings of the IEEE*, vol. 77, no. 7, pp. 941–981, 1989.

[13] J. B. Allen, "Short term spectral analysis, synthesis, and modification by discrete fourier transform," *IEEE Transactions on Acoustics, Speech and Signal Processing*, vol. ASSP-25, no. 3, pp. 235–238, 1977.